Decomposition of the scattering amplitude into shadow and surface components with inclusion of spin-orbit coupling

Germán Melo[*]
Instituto de Física, Universidad de Antioquia, AA. 1226, Medellín, Colombia

Jorge David[†]
Departamento de Ciencias Básicas-Ingeniería Física, Universidad Eafit, AA. 3300, Medellín, Colombia

Albeiro Restrepo[‡]
Grupo de Química-Física Teórica, Instituto de Química, Universidad de Antioquia, AA. 1226, Medellín, Colombia
(Received 7 March 2008; revised manuscript received 27 July 2008; published 29 September 2008)

We propose a decomposition of the scattering amplitude into shadow and surface components for proton scattering against calcium isotopes as targets at 21 MeV. We account for spin-orbit coupling effects for the optical potential in the nonrelativistic limit. Our calculations show very good agreement with experimental trends.

DOI: 10.1103/PhysRevC.78.034611 PACS number(s): 25.40.Cm, 03.65.Nk, 24.10.Ht

I. INTRODUCTION

In 1993, da Silveira and coworkers [1] proposed a decomposition of the scattering amplitude into shadow and surface components for the qualitative understanding of angular distributions in elastic collisions between ions and neutron-rich nuclei. The decomposition proposed allows the isolation of the contributions from the nuclear attraction while neglecting spin effects. The work by da Silveira decomposes the general Eq. (1) into Eqs. (3) and (4) according to the scheme of Eq. (2), that is,

$$f(\theta) = \frac{1}{2ik}\sum_{\ell=0}^{\infty}(2\ell+1)(e^{2i\Delta_\ell}-1)P_\ell(\cos\theta), \tag{1}$$

$$f(\theta) = f_{\text{shad}}(\theta) + f_{\text{surf}}(\theta), \tag{2}$$

with

$$f_{\text{shad}} = \frac{1}{2ik}\sum_{\ell=0}^{\infty}(2\ell+1)(\eta_\ell\, e^{2i\sigma_\ell}-1)P_\ell(\cos\theta), \tag{3}$$

and

$$f_{\text{surf}} = \frac{1}{2ik}\sum_{\ell=0}^{\infty}(2\ell+1)\eta_\ell\, e^{2i\sigma_\ell}(e^{2i\delta_\ell}-1)P_\ell(\cos\theta), \tag{4}$$

where σ_ℓ is the Coulomb phase shift, and $\delta_\ell = \text{Re}\Delta_\ell - \sigma_\ell$. The shadow amplitude is interpreted by da Silveira and coworkers as the scattering amplitude of incident particles interacting via the Coulomb force with an absorbing nonreflective target, whose opacity is given in ℓ space by η_ℓ, according to the strong absorption model (SAM) by Blair.

The surface amplitude term has significant contributions in a narrow window centered at $\ell \approx \ell_0$. As a consequence of the extended Babinet principle [2], the oscillations of $|f_{\text{surf}}(\theta)|^2$ and $|f_{\text{shad}}(\theta)|^2$ must be out of phase with respect to each other. In this work, we present a methodology for the decomposition of the dispersion amplitude that accounts for spin effects. We applied our methodology to studying the scattering between protons and calcium isotopes in the 21 MeV regime in the nonrelativistic limit.

II. RESULTS AND DISCUSSIONS

Following the optical model proposed by Melkanoff [3], which includes spin-orbit coupling, the two dispersion amplitudes for the collisions between spin 0 and spin 1/2 particles are given by

$$A(\theta) = f_c(\theta) + k^{-1}\sum_{\ell=0}^{\infty} e^{2i\sigma_\ell}\left[(\ell+1)C_\ell^{\ell+1/2} + \ell C_\ell^{\ell-1/2}\right] \times P_\ell(\cos\theta), \tag{5}$$

$$B(\theta) = (ik)^{-1}\sum_{\ell=1}^{\infty} e^{2i\sigma_\ell}\left[C_\ell^{\ell+1/2} - C_\ell^{\ell-1/2}\right]P_\ell^1(\cos\theta), \tag{6}$$

with

$$C_\ell^j = -\frac{i}{2}\left[e^{2i\delta_\ell^j}-1\right]. \tag{7}$$

The amplitude expansion coefficients C_ℓ^j and the imaginary part of the complex nuclear shifts $|\eta_\ell^j|$ are related by

$$C_\ell^j = \frac{1}{2i}\left[|\eta_\ell^j| e^{2i\text{Re}\delta_\ell^j}-1\right]. \tag{8}$$

Here, η_ℓ^j is the reflection coefficient and $|\eta_\ell^j| = e^{-2\text{Im}\delta_\ell^j}$. The analytical scattering amplitude for the Coulomb potential is

$$f_c(\theta) = \frac{1}{2ik}\sum_{\ell=0}^{\infty}(2\ell+1)[e^{2i\sigma_\ell}-1]P_\ell(\cos\theta), \tag{9}$$

[*]gmelo@elpoli.edu.co
[†]jdavidca@eafit.edu.co
[‡]albeiro@matematicas.udea.edu.co

TABLE I. Nonrelativistic optical model parameters. The energies (T_p, V, W, W_I, $V_{\rm ex}$, $V_{\rm so}$) are given in MeV, and distances (r_0, a_0, $r_{\rm so}$, $a_{\rm so}$ r_I, a_I, $r_{\rm ex}$, $a_{\rm ex}$) in fm.

Process	T_p	V	r_0	a_0	W	W_I	$r_{\rm so}$
p-^{40}Ca	21.0	52.14	1.155	0.747	0.0	7.85	0.959
p-^{42}Ca	21.0	55.57	1.112	0.764	0.0	8.13	1.066
p-^{44}Ca	21.0	52.86	1.142	0.722	0.0	8.87	1.047
p-^{48}Ca	21.0	54.82	1.147	0.795	0.0	9.69	0.833
Process	r_I	a_I	$V_{\rm so}$	$a_{\rm so}$	$V_{\rm ex}$	$r_{\rm ex}$	$a_{\rm ex}$
p-^{40}Ca	1.265	0.541	3.19	0.558	0.009	1.001	0.302
p-^{42}Ca	1.266	0.621	3.85	0.660	−0.008	0.844	0.124
p-^{44}Ca	1.286	0.602	6.16	0.791	0.032	0.901	0.228
p-^{48}Ca	1.333	0.541	6.52	0.724	0.0	–	–

where σ_ℓ is the Coulomb phase shift and $\eta = Z_1 Z_2 e^2/\hbar v$ is the Sommerfeld parameter. The differential cross section is calculated as

$$\sigma(\theta) = |A(\theta)|^2 + |B(\theta)|^2. \tag{10}$$

The second term in Eq. (10) gives a negligible contribution to the cross section, therefore it is eliminated from further calculations. Replacing Eqs. (8) and (9) into Eq. (5), we obtain

$$A(\theta) = \frac{1}{2ik}\sum_{\ell=0}^{\infty}[(\ell+1)|\eta_{\ell+1/2}|e^{2i\sigma_\ell}\, e^{2i{\rm Re}\delta_{\ell+1/2}} + \ell|\eta_{\ell-1/2}|e^{2i\sigma_\ell} e^{2i{\rm Re}\delta_{\ell-1/2}} - (2\ell+1)] \times P_\ell(\cos\theta). \tag{11}$$

Breaking Eq. (11) into two components

$$A(\theta) = \frac{1}{2ik}\sum_{\ell=0}^{\infty}\left[\left(\ell+\frac{1}{2}\right)|\eta_{\ell+1/2}|e^{2i\sigma_\ell} + \left(\ell+\frac{1}{2}\right)|\eta_{\ell-1/2}|e^{2i\sigma_\ell} - (2\ell+1)\right]P_\ell(\cos\theta) + \frac{1}{2ik}\sum_{\ell=0}^{\infty}\Bigg[(\ell+1)|\eta_{\ell+1/2}|e^{2i\sigma_\ell}\, e^{2i{\rm Re}\delta_{\ell+1/2}} + \ell|\eta_{\ell-1/2}|e^{2i\sigma_\ell}\, e^{2i{\rm Re}\delta_{\ell-1/2}} - \left(\ell+\frac{1}{2}\right)|\eta_{\ell+1/2}|e^{2i\sigma_\ell} - \left(\ell+\frac{1}{2}\right)|\eta_{\ell-1/2}|e^{2i\sigma_\ell}\Bigg]P_\ell(\cos\theta), \tag{12}$$

by writing Eq. (12) in the form $A(\theta) = A_{\rm shad}(\theta) + A_{\rm surf}(\theta)$, the second summation represents the surface component. Some algebra leads to

$$A_{\rm shad}(\theta) = \frac{1}{2ik}\sum_{\ell=0}^{\infty}(2\ell+1)\left[\frac{e^{2i\sigma_\ell}}{2}(|\eta_{\ell+1/2}| + |\eta_{\ell-1/2}|) - 1\right] \times P_\ell(\cos\theta). \tag{13}$$

Not taking into account spin effects in Eq. (12) reduces it to Eqs. (3) and (4). We used Numerov's algorithm [4,5] to numerically solve the radial part of Schrödinger's equation in order to obtain the C_ℓ^j, which contain the complex phase shifts δ_ℓ^j. In Schrödinger's equation, we used the optical-model potential (OMP) for proton-Ca isotopes proposed by Frahn [6]:

$$U(r) = V_c(r) - Vf(x_0) + i4a_I W_I \frac{d}{dr}f(x_I) - iWf(x_I) + (V_{\rm so} + iW_{\rm so})\frac{4}{r}\frac{df(x_{S0})}{dr}\mathbf{S}\cdot\mathbf{L} - V_{\rm ex}(-1)^\ell f(x_{\rm ex}). \tag{14}$$

When decomposing Eq. (12) into shadow and surface components, $A_{\rm surf}$ contains the real part of the phase shifts, which in turn are related to the surface effects, while the imaginary part of the phase shifts is exclusively placed on the $A_{\rm shad}$ term in Eq. (13).

The optical potential contains a total of 14 parameters, 8 are geometrical (r_0, a_0, r_I, a_I, $r_{\rm so}$, $a_{\rm so}$, $r_{\rm ex}$, $a_{\rm ex}$), and the remaining 6 (V, W, W_I, $V_{\rm so}$, T_p, $V_{\rm ex}$) are included to account for the dynamics of the process. It can be noticed from Table I that the W_I and r_I parameters increase with the A of the isotope and therefore are related to skin effects. The imaginary component of the potential is responsible for the absorption of incident particles whose contributions are included in the δ_ℓ^j associated to the shadow component. This shadow component dominates the Coulomb region and exhibits a Fraunhofer diffraction pattern that resembles the optical shadowed regions [7]; the real part of the optical nuclear potential is associated with the surface component [8]. The parameters in the potential are adjusted to give the best fit to the experimental data, using standard χ^2 minimization procedures as described in the paper by McCamis and coworkers [9]. Table I shows the parameters given in Ref. [9] for the potential (14); they used a dispersive optical-model analysis (DOMA) in which V_c is the electrostatic Coulomb potential and represented by the potential for a uniformly charged sphere as

$$V_c = \begin{cases} \frac{ZZ'e^2}{2R}\left[3 - \left(\frac{r}{R}\right)^2\right], & r \leqslant R, \\ ZZ'e^2/r, & r > R. \end{cases} \tag{15}$$

Here R is the Coulomb radius $R = r_c A^{1/3}$, and r_c is the radius parameter as determined from electron scattering experiments. Values given by Frosch *et al.* are 1.316, 1.306, 1.285, and 1.240 fm for ^{40,42,44,48}Ca, respectively [10]. The radial form

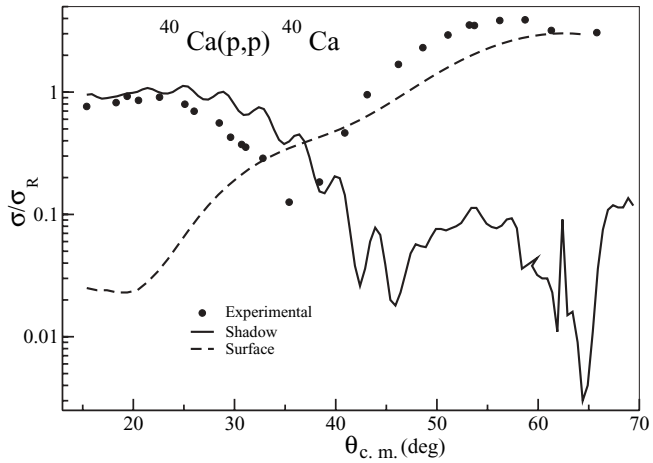

FIG. 1. 21 MeV proton scattering against ^{40}Ca targets. Experimental points provided by Van Oers [12].

factors are Woods-Saxon functions

$$f(x_a) = [1 + \exp(x_a)]^{-1}, \tag{16}$$

with

$$x_a = \frac{r - r_a A^{1/3}}{a_a}. \tag{17}$$

In calculations of the Coulomb phase shifts, we used the relationship [11]

$$\sigma = \sigma_0 + \sum_{s=1}^{\ell} \tan^{-1}\left(\frac{\eta}{s}\right), \tag{18}$$

where σ_0 may be approximated for all η by

$$\sigma_0 = -\eta + \frac{\eta}{2}\ln(\eta^2 + 16) + \frac{7}{2}\tan^{-1}\left(\frac{\eta}{4}\right) - \left[\tan^{-1}\eta + \tan^{-1}\left(\frac{\eta}{2}\right) + \tan^{-1}\left(\frac{\eta}{3}\right)\right]$$

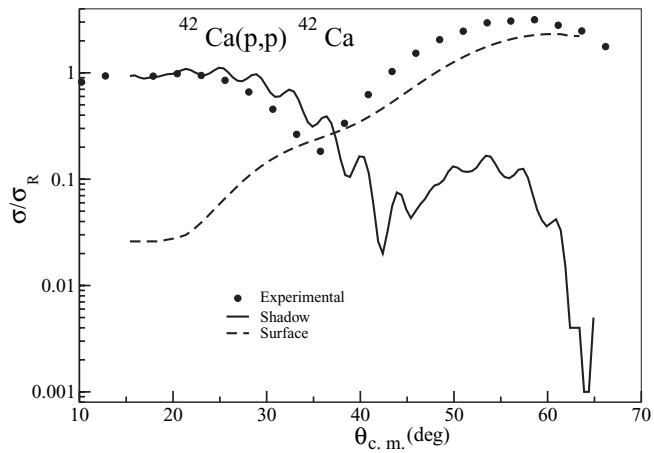

FIG. 2. 21 MeV proton scattering against ^{42}Ca targets. Experimental points provided by Van Oers [12].

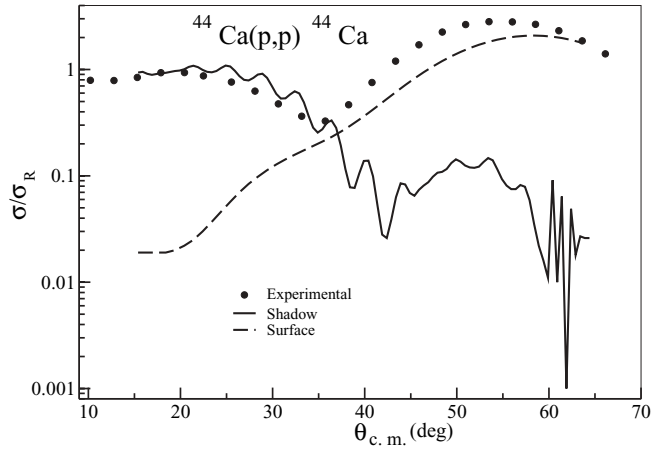

FIG. 3. 21 MeV proton scattering against ^{44}Ca targets. Experimental points provided by Van Oers [12].

$$-\frac{\eta}{12(\eta^2+16)}\left[1 + \frac{1}{30}\frac{(\eta^2-48)}{(\eta^2+16)^2} + \frac{1}{105}\frac{(\eta^4 - 160\eta^2 + 1280)}{(\eta^2+16)^4}\right]. \tag{19}$$

Figure 1 shows comparative results for the calculation of $|A_{\text{shad}}(\theta)|^2$ and $|A_{\text{surf}}(\theta)|^2$ against experimental points provided by Van Oers [12] for the scattering of protons with ^{40}Ca targets at 21 MeV. Figures 2, 3, and 4 show the scattering of 21 MeV protons when colliding with ^{42}Ca, ^{44}Ca, and ^{48}Ca, respectively.

It is observed from Figs. 1–4 that the Coulomb region is better described by the shadow component, while the surface component adequately describes the experimental behavior beyond the Coulomb region. Since the repulsive Coulomb potential lowers the nuclear attraction effects, we studied proton scattering against target nuclei with equal Z, so we effectively obtained information about neutron effects on the surface; we used the parameters of Ref. [9] for the optical potential. The correct behavior of our decomposition

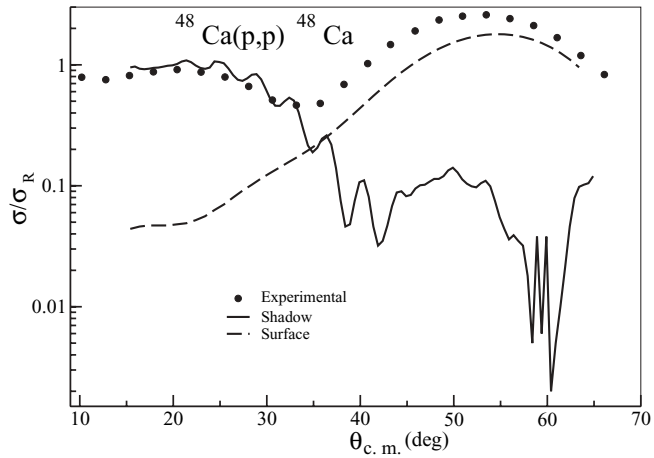

FIG. 4. 21 MeV proton scattering against ^{48}Ca targets. Experimental points provided by W. T. H. Van Oers [12].

was tested by modifying the real part and noticing that only the surface component was changed [13], leaving the shadow term unaltered; in this way, we were able to study skin effects. Skin effects can also be studied via alternative SAM parametrizations, such as those proposed by McIntyre *et al*. [14] and Franh and Venter [15] among others; in those methodologies, the functions vary softly and reduce the ambiguities of the optical potential; the surface transparency could be treated via DOMA [16].

III. CONCLUSIONS

In the present work, we study the scattering amplitude for proton collisions against calcium isotopes in the 21 MeV regime with the inclusion of spin effects. In the Coulomb region, tendencies are $|A_{\text{shad}}(\theta)|^2/\sigma_R \to 1$ and $|A_{\text{surf}}(\theta)|^2/\sigma_R \to 0$ as θ decreases, in agreement with previous reports. The shadow component, written as a function of the imaginary part of the phase shifts only, dominates the Coulomb region where a Fraunhofer-like diffraction pattern is observed; the surface component contains the real part of the phase shifts linked to surface effects. Inclusion of spin-orbit coupling in the potential allows us to calculate phase shifts. Such an approach could be used to study other effects such as the *p-n* interactions.

ACKNOWLEDGMENTS

The authors thank Manuel Páez of the Instituto de Física, Universidad de Antioquia, who wrote and provided the code used to obtain the nuclear phase shift calculations. We also thank W. T. J. Van Oers for providing us with all the experimental data, and Jorge G. Hirsch for useful discussions of the manuscript.

[1] R. da Silveira, S. Klarsfeld, A. Boukour, and Ch. Leclercq-Willain, Phys. Rev. C **48**, 468 (1993).
[2] R. da Silveira, Phys. Lett. **B264**, 248 (1991).
[3] M. A. Melkanoff, J. Raynal, and T. Sawada, *Nuclear Optical Model Calculations in Computational Physics*, Vol. 6 (Academic Press, New York, 1966).
[4] S. E. Koonin and D. C. Meredith, *Computational Physics*, FORTRAN version (Addison-Wesley, New York, 1990).
[5] A. C. Allison, J. Comput. Phys. **6**, 378 (1970).
[6] W. E. Frahn, *Fundamentals in Nuclear Theory* (IAEA,Vienna, 1967).
[7] J. S. Blair, Phys. Rev. **115**, 928 (1959).
[8] W. Tornow and J. P. Delaroche, Phys. Lett. **B210**, 26 (1988) .
[9] R. H. McCamis, T. N. Nasr, J. Birchall, N. E. Davison, W. T. H. van Oers, P. J. T. Verheijen, R. F. Carlson, A. J. Cox, B. C. Clark, E. D. Cooper, S. Hama, and R. L. Mercer, Phys. Rev. C **33**, 1624 (1986).
[10] R. F. Frosch, R. Hofstadter, J. S. McCarthy, G. K. Nöldeke, K. J. Van Oostrum, M. R. Yearian, B. C. Clark, R. Hertman, and D. G. Ravenhall, Phys. Rev. **174**, 1380 (1968).
[11] I. E. McCarthy, *Introduction to Nuclear Theory* (Wiley, New York, 1968).
[12] W. T. H. Van Oers (private communication).
[13] N. Austern, Ann. Phys. (NY) **15**, 299 (1961).
[14] J. A. McIntyre, K. H. Wang, and L. C. Becker, Phys. Rev. **117**, 1337 (1960).
[15] W. E. Frahn and R. H. Venter, Ann. Phys. (NY) **24**, 243 (1963).
[16] W. Tornow, Z. P. Chen, and J. P. Delaroche, Phys. Rev. C **42**, 693 (1990).